Revista Sul-Americana de Engenharia Estrutural
ISSN 2316-2457

A comparison study between seven procedures to predict vortex-induced vibrations on industrial chimneys

Grala, P.[1], Loredo-Souza, A. M.[2], Rocha, M. M.[3]

Abstract

Structures like towers and industrial chimneys are quite vulnerable to the vortex shedding phenomenon, due to their slenderness and non-aerodynamic form. Furthermore, due to their low structural damping, these structures are also more likely to reach large displacement amplitudes, which is caused by the lock-in effect. Although these structures are considered simple from the structural and aerodynamic viewpoints, the study of crosswind vibrations in these structures is quite complicated, as it involves the interaction of complex topics of fluid and structural mechanics, turning a reliable determination of the structural response into one of the most complicated problems in Wind Engineering. Because of that, this study aimed to compare some methods for predicting the response due to the vortex shedding phenomenon using full scale data from industrial chimneys. The chosen methods, which are exposed in codes and standards like Eurocode, National Building Code of Canada and CICIND Model Code for Steel Chimneys, derive from the Ruscheweyh's correlation length model and the Vickery & Basu's spectral mathematical model. In addition, these methods are also compared to three proposals made for the Brazilian Wind Code. This study concludes that the methods based on the Vickery and Basu's model work better for large displacement amplitudes.

Keywords: vortex shedding; industrial chimneys; dynamic response; vortex-induced vibrations; wind codes.

[1] Corresponding author, Ph.D. Candidate in the Department of Structural Engineering at Universidade Federal do Rio Grande do Sul, E-mail: pedro@egrala.com.br
[2] Professor at Universidade Federal do Rio Grande do Sul, E-mail: acir@ufrgs.br
[3] Professor at Universidade Federal do Rio Grande do Sul, E-mail: mmrocha@ufrgs.br

http://dx.doi.org/10535/rsaee.v15i2.7245

1. Introduction

Cross-wind forces caused by the vortex shedding phenomenon have been considered as a significant excitation mechanism for towers and chimneys. In some situations, the magnitude of cross-wind forces defines design specifications. Although these structures are considered simple from the structural and aerodynamic viewpoints, the determination of their structural response, even after some decades of study, is considered one of the most complicated problems in Wind Engineering.

During the 1980 decade the two most accepted models by the scientific community were proposed, which are the Ruscheweyh's correlation length model, and Vickery & Basu's spectral mathematical model. Both models consider motion-induced loads, but the way each model takes aeroelastic effects into account differs considerably. The first model often underestimates the displacement of the top of the structures when it has a small mass·damping relation (small Scruton number), but the second one overestimates it. Regarding small amplitude vibrations, both models work similarly.

Being incapable of reaching ultracritical Reynolds numbers, wind tunnels must use simulation techniques in order to obtain the desired flow. Therefore it is necessary to get measurements from prototypes in order to validate analytical methods, 42 structures (with full-scale measurements) were chosen for comparison with the predicted results. Most have reached large amplitude displacements (>5% of their diameter) and are not affected by the group effect. All have circular cross-section.

The Eurocode's Method I (EM-I) and the first proposal for the Brazilian Wind Code (BWC-I) are based on Ruscheweyh's model. The Eurocode adopts an identical procedure, but BWC-I brings some simplifications. Based on the spectral model, the CICIND Method, the NBC of Canada (NBCC), the Eurocode's Method II (EM-II) and the 2nd and 3rd proposal for the Brazilian Wind Code (BWC-II and BWC-III, respectively) are compared. From all of these seven methods, only NBCC and BWC-II do not apply to structures with small mass·damping relation (small Scruton number).

In order to simplify things, the methods presented in this paper consider only coefficients for circular cross-section and that the wind velocity V is always equal or under the critical velocity V_{cr}. Besides, it is considered that all structures are vibrating in their fundamental frequency, and that they all have a Strouhal number St equal to 0,2.

It is hoped that the considerations made in this paper could be useful to the engineering community when choosing the most suitable method for problems caused by cross-wind vibrations.

2. The vortex shedding phenomenon

In many non-aerodynamic bodies, like chimneys, towers and even some high-rise buildings, alternated vortex may shed, which have a well-defined frequency. These vortex are called Kármán vortex and create periodical forces in the cross-wind direction. Doing a vector analysis, the cross-wind direction forces occur in the frequency of each pair of vortex, while the forces in the along-wind direction occur in the frequency of a single vortex. These forces tend to produce oscillations in the direction they act. However, along-wind forces are small comparing to across-wind forces, and in a fluid like the air, oscillations in the flow direction rarely occur. Even the circular cylinder being the most studied section, this phenomenon may occur in other sections, like triangular, rectangular and other sections with sharp corners.

For a well-defined vortex shedding phenomenon occurrence on a structure, according to Blessmann (2005), its section should be curved or polygonal and it must have a considerable slenderness. Also, it is necessary a great shedding correlation over the whole body and the flow should be almost smooth. In practice, there are many causes that could prevent the vortex shedding correlation, like the wind profile or the diameter variation. According to Dyrbye and Hansen (1997), the pattern of a flow with only a vortex shedding frequency is idealized, which in practice does not happen due to the air turbulence.

The Strouhal number St is one of the most important parameters in the vortex shedding analysis. It depends on the shape of the structure, on the movement of the body, on the superficial roughness, on the Reynolds number and on the flow characteristics. This parameter states a relation between the frequency of the shedding of one pair of vortex f_s, a characteristic dimension of the structure (in the case of a tower or chimney, the diameter d) and the wind velocity V. This relation may be observed in Eq. (1):

$$St = \frac{f_s\, d}{V} \qquad (1)$$

When using the natural frequency of the structure f_n and the suitable St for the cross-section, Eq. (1) gives the critical velocity V_{cr}, which is the velocity in which the phenomenon starts. Another parameter of great importance is the Scruton number Sc. This parameter is known as mass·damping parameter, and states a relation between the mass of the structure and the mass of the flow in which the structure is immersed. The Eq. (2) shows the Scruton number:

$$\mathrm{Sc} = \frac{4\pi\, \mathrm{m_e}\, \varsigma_\mathrm{e}}{\rho\, \mathrm{d}^2} \qquad (2)$$

In which m_e is the equivalent mass per unit length, as defined in Eq. (3); ς_e is the critical structural damping ratio; ρ is the fluid's specific mass, the air in this case.

$$\mathrm{m_e} = \frac{\int_o^h \mathrm{m(z)} \varphi^2(\mathrm{z})\, \mathrm{dz}}{\int_o^h \varphi^2(\mathrm{z})\, \mathrm{dz}} \tag{3}$$

In which h is the total height of the structure; $m(z)$ is the mass per unit length; $\varphi(z)$ is the mode shape of the structure. Another important parameter is the Reynolds number, that consists in the ratio of the inertial forces and the fluid's viscosity. The Reynolds number Re is given by Eq. (4), in which ν is the kinematic viscosity of the fluid.

$$\mathrm{Re} = \frac{\mathrm{V\, d}}{\nu} \tag{4}$$

2.1 The lock-in effect

The movement of the cylinder exerts some control over the shedding of vortices, causing not only the observation of oscillations in the critical velocity, but also in other velocities near V_{cr} (mainly higher velocities). This phenomenon is also known as capture, synchronization or lock-on. When the flow velocity increases or decreases, so that the vortex shedding frequency approaches the fundamental frequency of the structure, and the cylinder oscillates, the vortices begin to shed in the natural frequency of the structure, and according to Ruscheweyh (1994), f_s does not follow the Strouhal law anymore, being constant over a specific range of speeds.

The two models studied in this paper differ considerably in the way they consider the fluid-structure interaction. In the spectral model it is considered the action of two uncorrelated forces: the forces generated by vortex shedding considering the structure at rest, and the forces correlated to the movement or the aerodynamic damping forces. These two last forces are linear function and self-limited by the displacement. In the correlation length model, the excitation generated by the vortex shedding considering a steady structure is modeled as sinusoidal forces acting over a single cell of vortices located at the top of the structure. The fluid-structure interaction is considered by a non-linear and self-limited by the equivalent cell increase, depending on the vibration magnitude.

3. The predicting methods

3.1 The Eurocode's first method (EM-I)

The Eurocode (2010) states that for circular cross-sections, the Strouhal number is equal to 0,18, but since it is a comparative study and that the Strouhal number affect directly in the response prediction, all structures will have the same Strouhal number of 0,2. The maximum displacement may be calculated following Eq. (5):

$$\frac{\hat{y}}{d} = \frac{1}{St^2}\frac{1}{Sc} K_\varphi K_w C_{lat} \quad (5)$$

In which $\hat{y}$ is the peak response of the top of the structure; K_φ is the constant of the mode shape, equal to 0,133 for $\varphi = (z/h)^2$, which is the chosen modal shape for towers and chimneys; K_w is the effective correlation length factor; C_{lat} is the lift force coefficient, given by Figure 1. It is also noted that in this study is considered that $C_{lat} = C_{lat,0}$. The Eurocode (2010) provides a reduction for $C_{lat,0}$ depending on the location wind speed. Since we cannot compare the location wind speed with the critical wind speed, we have chosen not to reduce the lift coefficient.

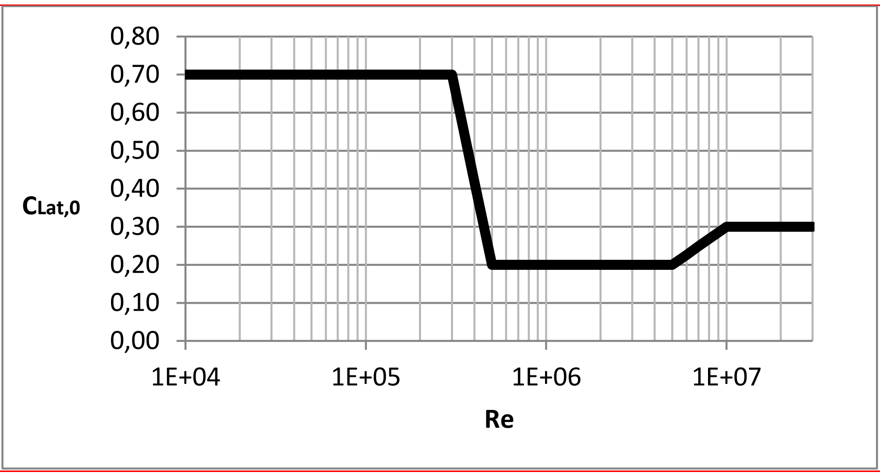

Figure 1: Lift coefficient according to the Eurocode (2010).

The effective correlation length factor for structures like towers and chimneys may be obtained by Eq. (6):

$$K_w = 3\,\frac{L_p/d}{\lambda}\left[1 - \frac{L_p/d}{\lambda} + \frac{1}{3}\left(\frac{L_p/d}{\lambda}\right)^2\right] \quad (6)$$

In which L_p is the correlation length, according to Table 1; λ is the slenderness ratio h/d.

Table 1: Correlation length versus vibration amplitude.

$\hat{y}/d$	L_p/d
$\hat{y}/d \leq 0,1$	6
$0,1<\hat{y}/d<0,6$	$4,8 + 12\,\hat{y}/d$
$\hat{y}/d \geq 0,6$	12

This is an iterative method, so, in order to obtain the response prediction, it is necessary to do the following procedure: adopt $L_p/d = 6$, calculate K_w and $\hat{y}/d$. Recalculate L_p/d and redo the process until $\hat{y}/d$ converge.

3.2 *The first proposal for the Brazilian Wind Code (BWC-I)*

This proposal is based on Ruscheweyh's model and is exposed in Blessmann (2005) and revised in Paluch (1999). This proposal considers different Strouhal numbers for different Reynolds numbers, but for purpose of comparison we are only considering Strouhal equal to 0,2. The only difference between this method and the Eurocode first method is in the coefficients L_p (Eq. 7), K_w (Eq. 8) and C_{lat}. For $Re \leq 2 \cdot 10^5$, $C_{lat} = 0{,}6$; for $Re > 2 \cdot 10^5$, $C_{lat} = 0{,}2$. Another difference is that the iteration starts in $L_p = 2$.

$$\frac{L_p}{d} = 12 - 10e^{-4\hat{y}/d} \tag{7}$$

$$K_w = 1 - \left(1 - \frac{L_p/d}{\lambda}\right)^3 \tag{8}$$

3.3 *The NBC of Canada method (NBCC)*

This code procedure was the first made based on the Vickery & Basu's model (Vickery and Basu 1983a; 1983b). The 1985 version of de code was chosen, because the new one does not have a procedure to predict the response of chimneys and towers due to the vortex shedding phenomenon anymore. The NBCC (1985) procedure also varies the Strouhal number with Reynolds, but it is only considered Strouhal equal to 0,2 in this study. This procedure is not capable to quantify the displacement (or force) in structures with small Scruton numbers, because it only works with structures in the forced vibration zone with small amplitudes.

Also, it is necessary to take note that this method gives the answer in terms of the equivalent force in the top third of the structure F and not the response in terms of displacement, as shown in Eq. (9):

$$F = \frac{C}{\sqrt{\lambda}\sqrt{\varsigma_e - K_a \frac{\rho\, d^2}{m_e}}} \frac{1}{2} \rho\, d\, V^2 \tag{9}$$

Where C is a parameter that depends on C_{lat}, St, L_p, the turbulence and the peak factor g_y; K_a is a parameter that represent the aerodynamic damping. It is necessary to note that this code procedure considers the average mass over the top third of the structure instead of m_e. It is a simplification that changes the response just a little, and since we do not have all the data from the analyzed chimneys (including the mass distribution over the tower) we will consider as m_e in this procedure.

Since Eq. (9) offers the response in terms of F, we need to convert the equation. Considering that in a single degree of freedom system $F = (2\pi f_n)^2 m_e \hat{y}$ and that $f_n = St\, V_{cr}/d$, by substituting them in Eq. (9) is given the Eq. (10):

$$\frac{\hat{y}}{d} = \frac{C/3{,}158}{\sqrt{\lambda}\sqrt{\varsigma_e - K_a \frac{\rho d^2}{m_e}}} \frac{\rho d^2}{m_e} \tag{10}$$

The recommendations of this method are that, for most cases, $K_a = 0{,}6$ and that $C = 3$ for $\lambda > 16$, and $C = 3\sqrt{\lambda}/4$ for $\lambda < 16$. When $V_{cr} < 10$ m/s and $\lambda > 16$, $K_a = 1{,}2$ and $C = 6$. The NBCC (1985) also gives coefficients C and K_a for tapered structures.

3.4 The second proposal for the Brazilian Wind Code (BWC-II)

This proposal was made by Paluch (1999), considering the simplified method of Vickery and Basu, exposed in Vickery and Basu (1983a; 1983b). This proposal only works in the small amplitudes zone and also cannot be used to design structures with low Scruton numbers. The peak displacement of the top of the structure is given by Eq. (11):

$$\frac{\hat{y}}{d} = \frac{C}{\sqrt{\lambda}\sqrt{\varsigma_e - K_a \frac{\rho d^2}{m_e}}} \frac{\rho d^2}{m_e} \tag{11}$$

This procedure varies C and K_a with the ratio $\theta = d(h)/d(0)$. For $\theta > 0{,}5$, $C = 0{,}7$ and $K_a = 0{,}6$. Since this study does not use tapered structures in its comparative examples, the expressions for $\theta < 0{,}5$ are not shown.

As this proposal states that for $Re < 3 \cdot 10^6$, $K_a = 1{,}2$, when calculating Re it should also be considered that this procedure multiplies V_{cr} by 1,14.

3.5 The Eurocode's second method (EM-II)

This second method is based on Vickery and Basu's model. However, it takes into account the considerations made by Vickery and Basu (1983a; 1983b) regarding the large amplitudes vibration zone. Since this method works both in the forced vibration and in the large amplitudes zones, the peak factor should vary, and the peak response in terms of displacement is given by Eq. (12).

$$\frac{\hat{y}}{d} = g_y \frac{\sigma_y}{d} \tag{12}$$

Where σ_y is the standard deviation of the top displacement of the structure. For large amplitudes $g_y = \sqrt{2}$ and for small amplitudes $g_y = 3{,}9$. The Eurocode (2010) uses the expression proposed by Ruscheweyh and Sedlacek (1998) for the peak factor. This equation is shown in Eq. (13) and allows a smooth transition between the vibration zones.

$$g_y = \sqrt{2}\left\{1 + 1{,}2\tan^{-1}\left[0{,}75\left(\frac{Sc}{4\pi\, K_a}\right)^4\right]\right\} \tag{13}$$

The standard deviation of the displacement of the top of the tower is given by Eq. (14), complemented by the following Eqs. (15)-(16):

$$\frac{\sigma_y}{d} = \sqrt{c_1 + \sqrt{c_1^2 + c_2}} \tag{14}$$

$$c_1 = \frac{\alpha^2}{2}\left(1 - \frac{Sc}{4\pi\, K_a}\right) \tag{15}$$

$$c_2 = \frac{\rho\, d^2}{m_e}\frac{\alpha^2}{K_a}\frac{C^2}{St^4}\frac{1}{\lambda} \tag{16}$$

In which α means the normalized limit amplitude, which is 0,4 for structures like chimneys and towers. The coefficients C and K_a are shown on Table 2:

Table 2: Coefficients C and K_a for circular cross-section according to the Eurocode (2010).

Coefficient	$Re \leq 10^5$	$Re = 5 \cdot 10^5$	$Re \geq 10^6$
C	0,02	0,005	0,01
K_a	2	0,5	1
Obs: for intermediate Reynolds values, the coefficients vary with the logarithmic interpolation.			

3.6 The CICIND method

The CICIND method is almost the same comparing to the Eurocode's second method. The only difference between them is regarding the peak factor, the coefficients C and K_a, and the reduction factor for K_a based on the turbulence intensity I_1. The considered peak factor, according to CICIND (2002a) is equal to 1,5 when $\sigma_y/d > 0{,}04$ and equal to 4 when $\sigma_y/d < 0{,}04$. The Table 3 shows the coefficients C and K_a depending on the Reynolds number.

Table 3: Coefficients C and K_a for circular cross-section according to the CICIND (2002b).

Coefficient	$Re \leq 10^5$	$Re = 5 \cdot 10^5$	$Re \geq 10^6$
C	0,02	Log. interpolation	0,01

K_a	1,5	1	1
Obs: for intermediate Reynolds values, the coefficients vary with the logarithmic interpolation.			

Based on the turbulence intensity, the CICIND model code (2002b) propose a reduction of K_a, according to Eq. (17):

$$K_a(Re, I_1) = K_a(Re)\, K_v\, (I_1) \quad (17)$$

In which $K_v\ (I_1)$ is a coefficient that depends on the turbulence intensity. $K_v\ (I_1) = 1 - 3I_1$ when I_1 is equal to or less than 0,25 and $K_v\ (I_1) = 0{,}25$ for I_1 larger values. According to CICIND (2002b), the turbulence intensity is given by the following consideration: for open sea or smooth flat country without any obstacles $I_1 = 0$ for $V_{cr} \leq 10$ m/s and $I_1 = 0{,}1$ for $V_{cr} > 10$ m/s; for all other terrain categories $I_1 = 0$ for $V_{cr} \leq 7$ m/s and $I_1 = 0{,}1$ for $V_{cr} > 7$ m/s.

The CICIND (2002b) also gives a simplified equation for the design of most non-heavily damped chimneys with Scruton less than $4\,\pi\,K_a$. This consideration is given by Eq. (18):

$$\frac{\hat{y}}{d} = g_y \sqrt{2\,c_1} = g_y\, 0{,}4 \sqrt{1 - \frac{Sc}{4\pi\, K_a}} \quad (18)$$

3.7 The third proposal for the Brazilian Wind Code (BWC-III)

The third proposal for the Brazilian Wind Code is also based on the Vickery & Basu's model, but it is more like the Eurocode's second method and the CICIND method, because it considers the large amplitude vibrations. It is exposed in Grala (2016).

As on these two methods, the response of the structure in terms of displacement is given by Eq. (12), and the standard deviation of the displacement is given by Eq. (19):

$$\frac{\sigma_y}{d} = \sqrt{\frac{\alpha^2}{2}(1-K) + \sqrt{\frac{\alpha^4}{4}(1-K)^2 + \frac{\alpha^2 C^2 \rho\, d^3}{m_e\, K_a\, h\, St^4}}} \quad (19)$$

In which K is a damping parameter, being simply the ratio between structural and aerodynamic damping. K is given in Eq. (20). The parameters C and K_a are shown on Table 4, and both take into consideration their variation with Reynolds number and turbulence intensity (through the wind critical speed, as on the CICIND and NBC of Canada methods).

$$K = \frac{m_e\, \varsigma_e}{\rho\, d^2\, K_a} = \frac{Sc}{4\pi\, K_a} \quad (20)$$

Table 4: Coefficients C and K_a for circular cross-section for the BWC-III.

Re_{cr}	C		K_a	
	$V_{cr} < 11$	$V_{cr} \geq 11$	$V_{cr} < 11$	$V_{cr} \geq 11$
$Re \leq 2 \cdot 10^5$	0,0554	0,0261	2	1,1
$2 \cdot 10^5 < Re \leq 10^6$	0,1840 - 0,0286 log(Re)	0,0867 – 0,0135 log(Re)	1,2	0,6
$Re > 10^6$	0,0208	0,0098	1,2	0,6

For structures with $K \leq 0{,}95$, the Eq. (19) may be simplified to Eq. (21):

$$\frac{\sigma_y}{d} = \alpha \sqrt{(1 - K)} \tag{21}$$

For structures with $K \geq 1{,}05$, the Eq. (19) may be simplified to Eq. (22):

$$\frac{\sigma_y}{d} = \sqrt{\frac{C^2 \rho d^3}{m_e h K_a St^4 (K - 1)}} \tag{22}$$

The peak factor g_y is given by Eq. (23), which is a simplification of the Ruscheweyh and Sedlacek's peak factor proposal.

$$g_y = 1{,}4 + 1{,}6 \tan^{-1}(0{,}75 K^4) \tag{23}$$

4. Results

This chapter presents the application of each of the presented methods in 42 real structures, with full-scale data. The structures were chosen following the criterion of low Scruton values. Besides, the normalized displacement of the top of a large part of the chosen structures exceeds 5%, being this amount the upper limit of the forced vibration zone. In other words, a large part of the chosen structures suffered the lock-in effect.

The Table 5 shows a resume of the comparison among the 42 studied structures. It presents the values of the measured displacement of the top of the structures and compares with the predicted results obtained with each of the seven procedures shown in this paper.

In the columns 'Data – Measured' and 'Data – Observed' the values of the top deflection in function of their diameters are presented. The measured data were obtained by appropriate instruments, while the observed data were from structures without instrumentation. 'Scruton' refers to the Scruton number of that respective structure.

The columns 'Ruscheweyh – EM-I' and 'Ruscheweyh – BWC-I' show the normalized top displacement predicted by the correlation length model, which was adopted in the first Eurocode method and in the first proposal for the Brazilian Wind Code. It may be observed that the displacements predicted by these methods are much lower compared to the measured data. Only in 15 of the 42 cases the Eurocode's first method was in favor of safety, and only in 11 cases the first proposal for the BWC predicted with safety.

The columns included in ‘Vickery & Basu (small and large amplitudes)’ present the obtained results by the third proposal for the BWC, by the Eurocode’s second method and by the CICIND method. Respectively, each method gave 40, 39 and 37 predictions in favor of safety. It should be noted that in the two cases that BWC-III underestimated the response, the error rates were 1% and 3%, while in the other methods the predicted responses were 2,5 (EM-II) and 4 (CICIND) times less than the measured data.

In the columns situated under ‘Vickery & Basu (small amplitudes)’ it is possible to observe the incapacity of these methods in predicting the response of structures with low mass-damping rate. For the presented cases, for both methods, only two responses were predicted in safety.

The Table 5 only shows the summary of the measured and predicted responses. It is better to take a global look of how the methods work. In this table, cells in gray represent when the method is in favor of security.

Table 5: Summary of the measured and predicted responses.

Structure	Data			Ruscheweyh		V & B (large & small amplitudes)			V & B (small amplitudes)	
Number	Measured	Observed	Scruton	EM-I	BWC-I	BWC-III	EM-II	CICIND	NBCC	BWC-II
1	0,25	-	1,62	0,28	0,28	0,53	0,53	0,54	-	-
2	0,15	-	2,10	0,18	0,16	0,52	0,47	0,52	-	-
3	0,02	-	4,07	0,10	0,08	0,48	0,47	0,44	-	-
4	0,03	-	10,76	0,08	0,01	0,37	0,35	0,32	-	-
5	0,01	-	15,14	0,02	0,01	0,14	0,03	0,04	0,48	0,18
6	0,04	0,36	3,03	0,14	0,13	0,50	0,49	0,49	-	-
7	-	0,42	4,08	0,08	0,05	0,48	0,45	0,49	-	-
8	-	0,28	4,77	0,07	0,04	0,47	0,39	0,47	-	-
9	-	0,20	6,10	0,07	0,05	0,33	0,43	0,33	-	-
10	-	0,37	6,50	0,16	0,02	0,44	0,44	0,46	-	-
11	0,17	-	10,40	0,04	0,02	0,37	0,33	0,04	0,03	0,02
12	-	0,23	5,88	0,06	0,04	0,45	0,43	0,44	-	-
13	0,25	-	6,00	0,05	0,03	0,44	0,31	0,43	-	-
14	-	0,31	8,87	0,07	0,07	0,40	0,13	0,33	0,07	-
15	0,38	-	2,56	0,13	0,12	0,51	0,45	0,51	-	-
16	0,48	-	7,33	0,12	0,08	0,47	0,46	0,46	-	-
17	0,25	-	1,90	0,19	0,19	0,52	0,52	0,53	-	-
18	0,03	-	17,23	0,02	0,01	0,08	0,03	0,03	0,10	0,04
19	0,07	-	10,71	0,09	0,01	0,37	0,37	0,33	-	-
20	0,06	-	4,00	0,15	0,11	0,41	0,47	0,44	-	-
21	0,06	-	2,90	0,23	0,18	0,45	0,50	0,49	-	-
22	0,06	-	4,90	0,11	0,07	0,38	0,45	0,40	-	-
23	0,02	-	4,50	0,10	0,08	0,39	0,46	0,42	-	-
24	0,25	-	2,60	0,15	0,08	0,51	0,46	0,54	-	-
25	0,20	-	2,70	0,18	0,14	0,46	0,50	0,50	-	-
26	0,46	-	1,30	0,39	0,40	0,54	0,54	0,55	-	-

27	0,33	-	1,40	0,37	0,37	0,51	0,53	0,55	-	-
28	0,50	-	6,60	0,07	0,03	0,48	0,49	0,48	-	-
29	0,22	-	1,60	0,53	0,37	0,50	0,53	0,54	-	-
30	0,29	-	8,59	0,04	0,02	0,40	0,38	0,10	-	-
31	0,21	-	2,80	0,15	0,12	0,51	0,44	0,53	-	-
32	0,17	-	4,20	0,09	0,07	0,48	0,47	0,43	-	-
33	0,25	-	1,90	0,31	0,14	0,52	0,49	0,55	-	-
34	0,40	-	2,90	0,07	0,04	0,50	0,44	0,53	-	-
35	0,40	-	3,10	0,18	0,02	0,50	0,50	0,54	-	-
36	0,17	-	7,60	0,05	0,03	0,42	0,40	0,22	-	-
37	0,18	-	1,40	0,34	0,35	0,51	0,53	0,55	-	-
38	0,28	-	2,40	0,64	0,09	0,51	0,52	0,55	-	-
39	0,30	-	1,80	0,25	0,25	0,53	0,52	0,54	-	-
40	0,45	-	4,20	0,13	0,09	0,51	0,52	0,53	-	-
41	0,25	-	2,77	0,15	0,14	0,51	0,50	0,50	-	-
42	0,25	-	6,75	0,06	0,04	0,43	0,41	0,29	-	-

The reference for each presented structure follows: struct. (1) – Ruscheweyh (1994); struct. (2) – Ruscheweyh and Galemann (1996); struct. (3)-(8) – Frandsen (1979 *apud* Dyrbye and Hansen, 1997); struct. (9)-(10) – Ciesielski et al. (1992); struct. (11) – Basu (1983); struct. (12)-(14) and (17) and (38)-(40) – Hansen (1998); struct. (15)-(16) and (18)-(19) – Langer et al. (1996 *apud* Verboom and van Koten, 2010); struct. (20)-(23) – Nakagawa et al. (1963); struct. (24) – Scruton (1955 *apud* Pritchard, 1984); struct. (25)-(26) – Hirsch and Ruscheweyh (1975); struct. (27)-(28) and (31)-(32) and (37) and (41) – Pritchard (1984); struct. (29) – Ozker and Smith (1956 *apud* Pritchard 1984); struct. (30) – Dickey and Woodruff (1954 *apud* Pritchard 1984); struct. (33)-(35) – van Koten (1979 *apud* Pritchard 1984); struct. (36) and (42) – Zorilla (1972 *apud* Pritchard 1984).

5. Analisis and conclusions

From the analysis of the comparison results exposed on section 4, it is possible to observe that the correlation length model often underestimates the top displacement of the structure. As this model allows the design of low Scruton structures, it is not recommended its use without proper attention. For structures with Scruton number over 20, the response predictions are so reliable as those predicted with the Vickery & Basu model, because after this Scruton value, the vibration tend to be in the small amplitudes zone.

As stated before, the Vickery & Basu model can be used in two ways, one considering only in the forced vibration zone, and another considering the structure in both the forced and the large vibration zones. The NBCC and BWC-II allow the design only of high Scruton structures.
Therefore, a more embracing approach could be the use of the EM-II, the CICIND method and the BWC-III. These three methods obtained the best results, as seen in section 4, allowing the design of low Scruton structures with safety.

However, by looking at the exposed results, it is possible to conclude that these three methods overestimate the responses. This may not be true, because in some cases the phenomenon has not occurred completely or in its full magnitude during the observation period. The examples 2 (Ruscheweyh and Galemann 1996 and 15 (Langer et al. 1996 *apud* Verboom and van Koten 2010) are from the same structure, but observed at distinct periods. In example 2, $\hat{y}/d = 0{,}154$, while in example 15, $\hat{y}/d = 0{,}38$. The same structure was continuously observed by Galemann and Ruscheweyh (1992) between 1987 and 1990, being the peak response equal to $\hat{y}/d = 0{,}14$. This allows to conclude that the methods are not overestimating the response, since the lock-in effect can reach a top displacement of 40% of the diameter of the structure, even if this value was not measured in the determined observation period.

Acknowledgements

The authors acknowledge CAPES, Brazil, for the support to the first author during his Master and Ph.D. programs.

Appendix

This appendix shows the same structures that appear on Table 5. The difference is that the following Tables 6-12 present the structural characteristics of each structure. In these tables, cells in grey represent that those value were estimated.

Table 6: Measured and predicted response in detail for examples 1-6.

	Example	1	2	3	4	5	6
Properties of the structure and of the flow	me [kg/m]	340,00	87,00	885,70	241,29	782,60	1069,07
	ς	0,0019	0,0019	0,0022	0,0054	0,0094	0,0022
	Sc	1,62	2,10	4,07	10,76	15,14	3,03
	St	0,20	0,20	0,20	0,20	0,20	0,20
	d [m]	2,00	0,91	2,20	1,10	2,20	2,80
	h [m]	52,00	28,00	50,00	45,00	54,00	64,00
	λ	26,00	30,77	22,73	40,91	24,55	22,86
	f [Hz]	0,75	1,70	0,92	0,63	0,61	0,58
	Vcr [m/s]	7,50	7,74	10,12	3,47	6,71	8,12
	Re	1,05E+06	4,93E+05	1,56E+06	2,67E+05	1,03E+06	1,59E+06
	ρ [kg/m³]	1,26	1,26	1,26	1,26	1,26	1,26
y/d	Measured	0,25	0,15	0,02	0,03	0,01	0,04
	Observed						0,36
	EM-I	0,28	0,18	0,10	0,08	0,02	0,14
	BWC-I	0,28	0,16	0,08	0,01	0,01	0,13
	BWC-III	0,53	0,52	0,48	0,37	0,14	0,50
	EM-II	0,53	0,47	0,47	0,35	0,03	0,49
	CICIND	0,54	0,52	0,44	0,32	0,04	0,49
	NBCC	-	-	-	-	0,48	-
	BWC-III	-	-	-	-	0,18	-

Table 7: Measured and predicted response in detail for examples 7-12.

	Example	7	8	9	10	11	12
Properties of the structure and of the flow	me [kg/m]	494,00	389,47	200,35	136,34	5137,45	598,23
	ς	0,0048	0,0040	0,0048	0,0032	0,0032	0,0048
	Sc	4,08	4,77	6,10	6,50	10,40	5,88
	St	0,20	0,20	0,20	0,20	0,20	0,20
	d [m]	2,40	1,80	1,25	0,82	3,96	2,20
	h [m]	75,00	56,00	26,00	30,00	80,00	56,00
	λ	31,25	31,11	20,80	36,76	20,20	25,45
	f [Hz]	0,37	0,49	1,88	1,06	0,53	0,62
	Vcr [m/s]	4,44	4,41	11,75	4,32	10,49	6,82
	Re	7,46E+05	5,56E+05	1,03E+06	2,47E+05	2,91E+06	1,05E+06
	ρ [kg/m³]	1,26	1,26	1,26	1,26	1,26	1,26
y/d	Measured					0,17	
	Observed	0,42	0,28	0,20	0,37		0,23
	EM-I	0,08	0,07	0,07	0,16	0,04	0,06
	BWC-I	0,05	0,04	0,05	0,02	0,02	0,04
	BWC-III	0,47	0,47	0,33	0,44	0,37	0,45
	EM-II	0,45	0,39	0,43	0,44	0,33	0,43
	CICIND	0,49	0,47	0,33	0,46	0,04	0,44
	NBCC	-	-	-	-	0,03	-
	BWC-III	-	-	-	-	0,02	-

Table 8: Measured and predicted response in detail for examples 13-18.

	Example	13	14	15	16	17	18
Properties of the structure and of the flow	me [kg/m]	483,86	362,13	89,82	203,49	319,20	347,36
	ς	0,0032	0,0064	0,0024	0,0024	0,0024	0,0199
	Sc	6,00	8,87	2,56	7,33	1,90	17,23
	St	0,20	0,20	0,20	0,20	0,20	0,20
	d [m]	1,60	1,61	0,91	0,81	2,00	2,00
	h [m]	50,00	12,50	28,00	35,00	60,00	60,00
	λ	31,25	7,76	30,63	43,05	30,00	30,00
	f [Hz]	0,60	0,73	1,72	0,61	0,80	0,77
	Vcr [m/s]	4,80	5,88	7,86	2,49	8,02	7,70
	Re	5,38E+05	6,62E+05	5,03E+05	1,42E+05	1,12E+06	1,08E+06
	ρ [kg/m³]	1,26	1,26	1,26	1,26	1,26	1,26
y/d	Measured	0,25		0,38	0,48	0,25	0,03
	Observed		0,31				
	EM-I	0,05	0,07	0,13	0,12	0,19	0,02
	BWC-I	0,03	0,07	0,12	0,08	0,19	0,01
	BWC-III	0,44	0,40	0,51	0,47	0,52	0,08
	EM-II	0,31	0,13	0,45	0,46	0,52	0,03
	CICIND	0,43	0,33	0,51	0,46	0,53	0,03
	NBCC	-	0,07	-	-	-	0,10
	BWC-III	-	-	-	-	-	0,04

Table 9: Measured and predicted response in detail for examples 19-24.

	Example	19	20	21	22	23	24
Properties of the structure and of the flow	me [kg/m]	232,16	2184,84	1832,87	1365,59	1347,51	187,54
	ς	0,0048	0,0048	0,0045	0,0060	0,0051	0,0021
	Sc	10,71	4,00	2,90	4,90	4,50	2,60
	St	0,20	0,20	0,20	0,20	0,20	0,20
	d [m]	1,02	5,10	5,30	4,10	3,90	1,22
	h [m]	38,00	90,00	91,15	83,00	77,00	46,00
	λ	37,40	17,65	17,20	20,24	19,74	37,70
	f [Hz]	0,68	0,75	0,68	1,15	0,69	0,90
	Vcr [m/s]	3,45	19,13	17,89	23,58	13,49	5,49
	Re	2,46E+05	6,83E+06	6,64E+06	6,77E+06	3,68E+06	4,69E+05
	ρ [kg/m³]	1,26	1,26	1,26	1,26	1,26	1,26
y/d	Measured	0,07	0,06	0,06	0,06	0,02	0,25
	Observed						
	EM-I	0,09	0,15	0,23	0,11	0,10	0,15
	BWC-I	0,01	0,11	0,18	0,07	0,08	0,08
	BWC-III	0,37	0,41	0,45	0,38	0,39	0,51
	EM-II	0,37	0,47	0,50	0,45	0,46	0,46
	CICIND	0,33	0,44	0,49	0,40	0,42	0,54
	NBCC	-	-	-	-	-	-
	BWC-III	-	-	-	-	-	-

Table 10: Measured and predicted response in detail for examples 25-30.

	Example	25	26	27	28	29	30
Properties of the structure and of the flow	me [kg/m]	1975,35	567,00	631,14	35,01	765,00	970,00
	ς	0,0049	0,0021	0,0021	0,0030	0,0050	0,0060
	Sc	2,70	1,30	1,40	6,60	1,60	8,59
	St	0,20	0,20	0,20	0,20	0,20	0,20
	d [m]	6,00	3,00	3,05	0,40	4,88	2,60
	h [m]	145,00	74,00	72,00	36,00	91,50	76,00
	λ	24,17	24,67	23,61	90,00	18,75	29,23
	f [Hz]	0,50	0,70	0,80	0,40	1,00	0,60
	Vcr [m/s]	15,00	10,50	12,20	0,80	24,40	7,80
	Re	6,30E+06	2,21E+06	2,60E+06	2,24E+04	8,34E+06	1,42E+06
	ρ [kg/m³]	1,26	1,26	1,26	1,26	1,26	1,26
y/d	Measured Observed	0,20	0,46	0,33	0,50	0,22	0,29
	EM-I	0,18	0,39	0,37	0,07	0,53	0,04
	BWC-I	0,14	0,40	0,37	0,03	0,37	0,02
	BWC-III	0,46	0,54	0,51	0,48	0,50	0,40
	EM-II	0,50	0,54	0,53	0,49	0,53	0,38
	CICIND	0,50	0,55	0,55	0,48	0,54	0,10
	NBCC	-	-	-	-	-	-
	BWC-III	-	-	-	-	-	-

Table 11: Measured and predicted response in detail for examples 31-36.

	Example	31	32	33	34	35	36
Properties of the structure and of the flow	me [kg/m]	382,98	451,21	229,86	140,54	138,45	1298,94
	ς	0,0021	0,0030	0,0021	0,0021	0,0021	0,0049
	Sc	2,80	4,20	1,90	2,90	3,10	7,60
	St	0,20	0,20	0,20	0,20	0,20	0,20
	d [m]	1,68	1,80	1,58	1,00	0,96	2,90
	h [m]	43,50	46,00	60,00	60,00	75,00	76,00
	λ	25,89	25,56	37,97	60,00	78,13	26,21
	f [Hz]	0,50	0,90	0,50	0,60	0,80	0,70
	Vcr [m/s]	4,20	8,10	3,95	3,00	3,84	10,15
	Re	4,94E+05	1,02E+06	4,37E+05	2,10E+05	2,58E+05	2,06E+06
	ρ [kg/m³]	1,26	1,26	1,26	1,26	1,26	1,26
y/d	Measured	0,21	0,17	0,25	0,40	0,40	0,17
	Observed						
	EM-I	0,15	0,09	0,31	0,07	0,18	0,05
	BWC-I	0,12	0,07	0,14	0,04	0,02	0,03
	BWC-III	0,51	0,48	0,52	0,50	0,50	0,50
	EM-II	0,44	0,47	0,49	0,44	0,50	0,40
	CICIND	0,53	0,43	0,55	0,53	0,54	0,22
	NBCC	-	-	-	-	-	-
	BWC-III	-	-	-	-	-	-

Table 12: Measured and predicted response in detail for examples 37-42.

	Example	37	38	39	40	41	42
Properties of the structure and of the flow	me [kg/m]	310,71	116,31	223,31	164,87	300,00	780,00
	ς	0,0021	0,0021	0,0021	0,0021	0,0030	0,0050
	Sc	1,40	2,40	1,80	4,20	2,77	6,75
	St	0,20	0,20	0,20	0,20	0,20	0,20
	d [m]	2,14	1,00	1,60	0,90	1,80	2,40
	h [m]	55,00	40,00	40,00	65,00	43,00	56,00
	λ	25,70	40,00	25,00	72,22	23,89	23,33
	f [Hz]	1,10	0,70	1,30	0,30	1,00	0,83
	Vcr [m/s]	11,77	3,50	10,40	1,35	9,00	9,96
	Re	1,76E+06	2,45E+05	1,16E+06	8,51E+04	1,13E+06	1,67E+06
	ρ [kg/m³]	1,26	1,26	1,26	1,26	1,26	1,26
y/d	Measured	0,18	0,28	0,30	0,45	0,25	0,25
	Observed						
	EM-I	0,34	0,64	0,25	0,13	0,15	0,06
	BWC-I	0,35	0,09	0,25	0,09	0,14	0,04
	BWC-III	0,51	0,51	0,53	0,51	0,51	0,43
	EM-II	0,53	0,52	0,52	0,52	0,50	0,41
	CICIND	0,55	0,55	0,54	0,53	0,50	0,29
	NBCC	-	-	-	-	-	-
	BWC-III	-	-	-	-	-	-

References

Basu, R. I. (1983). Across-wind response of slender structures of circular cross-section to atmospheric turbulence. Ph.D. Thesis, The University of Western Ontario, London, Canada.

Blessmann, J. (2005). Introdução ao Estudo das Ações Dinâmicas do Vento. 2nd ed., Editora da UFRGS, Porto Alegre.

CICIND (2002a). Model Code for Steel Chimneys, Zurich.

CICIND (2002b). Model Code for Steel Chimneys, Commentaries and Appendices, Zurich.

Ciesielski, R., Gaczec, M., Kawecki, J. (1992). Observation results of cross-wind response of towers and steel chimneys, J. of Wind Eng. and Indust. Aerodynamics, v.43, p. 2205-2211.

Dickey, W. L., Woodruff, G. B. (1954). The vibrations of steel stacks, Proceedings of 80 ASCE Structures Congress.

Dyrbye, C., Hansen, S. O. (1997) Wind Loads on Structures. John Wiley & Sons, Chichester.

Eurocode 1 (2010). Actions on Structures – Part 1-4: General Actions – Wind Actions, EN 1991 – 1-4, The European Standard.

Frandsen, S. (1979). RISØ kontraktrapport: Tværsvingninger af stålskorstene, Feltmålinger.

Galemann, T., Ruscheweyh, H. (1992). Measurements of wind induced vibrations of a full scale steel chimney. J. of Wind Eng. and Indust. Aerodynamics, v. 41, p. 241-252.

Grala, P. (2016). Estudo das metodologias para o cálculo da resposta de estruturas cilíndrico circulares frente ao fenômeno de desprendimento de vórtices: proposta atualizada para a NBR-6123. M.Sc. Dissertation, Universidade Federal Rio Grande do Sul, Porto Alegre.

Hansen, S. O. (1998). Vortex-induced vibrations of line-like structures. CICIND Report, v.15, n. 1, p. 15-23.

Hirsch, G., Ruscheweyh, H. (1975). Full-scale measurements on steel chimney stacks. J. of Wind Eng, and Indust. Aerodynamics, v. 1, p. 341-347.

Langer, W., Ruscheweyh, H., Verwiebe, C. (1996). Untersuchung des Querschwingungsverhaltens von Original-Stahlschornsteinen. Forschungsbericht P230.

Nakagawa, K., Fujino, T., Arita, Y., Shima, T. (June 1963). An experimental study of aerodynamic devices for reducing wind-induced oscillatory tendencies of stacks. Wind Effects on Buildings and Structures, v. 16, Teddington.

National Research Council of Canada (NBC) (1985). Supplement to the National Building Code of Canada, Ottawa.

Ozker, M. S., Smith, J. O. (1956). Factors influencing the dynamic behaviour of tall stacks under the action of wind. ASME v. 78.

Paluch, M. J. (1999). Vibrações transversais por desprendimento de vórtices de torres e chaminés de concreto armado de seção transversal circular. Ph.D. Thesis, Universidade Federal Rio Grande do Sul, Porto Alegre.

Pritchard, B. N. (1984). Steel chimney oscillations: a comparative study of their reported performance versus predictions using existing design techniques. Eng. Str., v. 6, p. 315-323.

Ruscheweyh, H. (1994). Vortex excited vibrations. Wind-Excited Vibrations of Structures Springer-Verlag Wien, New York. Reference to a chapter in an edited book.

Ruscheweyh, H., Galemann, T. (1996). Full-scale measurements of wind-induced oscillations of chimneys. J. of Wind Eng. and Indust. Aerodynamics, v. 65, p. 55-62.

Ruscheweyh, H. and Sedlacek, G. (1998). Crosswind vibrations of steel stacks – critical comparison between some recently proposed codes. J. of Wind Eng. and Indust. Aerodynamics, v. 30, p. 173-183.

Scruton, C. (1955). Wind excited oscillations of tall stacks. Engineer 30.

Van Koten, H. (1979). Experiences with cross wind vibrations of towers and stacks. Symp. Practical Experiences with Flow-induced Vibrations, Karlsruhe.

Verboom, G. K., van Koten, H. (2010). Vortex excitation: three design rules tested on 13 industrial chimneys. J. of Wind Eng. and Indust. Aerodynamics, v. 98, p. 145-154.

Vickery, B. J., Basu, R. I. (1983a). Across-wind vibrations of structures of circular cross-sections. Part I. Development of a mathematical model for two-dimensional conditions. J. of Wind Eng. and Indust. Aerodynamics, v. 12, p. 49-73.

Vickery, B. J., Basu, R. I. (1983b). Simplified approaches to the evaluation of the across-wind response of chimneys. J. of Wind Eng. and Indust. Aerodynamics, v. 14, p. 153-166.

Zorilla, E. P. (1972). Determination of aerodynamic behaviour of cantilevered stacks and towers of circular cross section. ASME Publ. 71.